



# FMR linewidth and the crystallization processes in Co-based amorphous microwires

D.S. Chrischon<sup>a</sup>, F. Beck<sup>a</sup>, K.D. Sossmeier<sup>b</sup>, M. Carara<sup>a,\*</sup>

<sup>a</sup> Departamento de Física, Universidade Federal de Santa Maria (UFSM), Santa Maria, 97105-900 RS, Brazil

<sup>b</sup> Instituto Latino-Americano de Ciências da Vida e da Natureza, Universidade Federal da Integração Latino-Americana (UNILA), Foz do Iguaçu, 85867-970 PR, Brazil

## ARTICLE INFO

### Article history:

Received 19 November 2012

Available online 9 February 2013

### Keywords:

FMR linewidth

Damping parameter

Magnetization relaxation

## ABSTRACT

The ferromagnetic resonance (FMR) technique has been used for many years as a tool to characterize the dynamic magnetic properties of bulk, thin film magnetic materials and microwires. Also, the FMR linewidth is associated to the dissipative processes involved on the magnetization dynamics. Such dissipative channels may be separated in two groups: intrinsic and extrinsic ones. While the first one is related mainly to the Landau–Lifshitz (LL) and eddy-currents damping mechanisms, the second one take in to account contributions coming from the inhomogeneities in the sample. Each one of these relaxation processes contributes to the FMR linewidth in a different frequency and/or magnetic field range and they can be separated by an appropriate FMR linewidth measurement. This work presents FMR measurements, obtained by the impedance method, ranging from 100 KHz to 1.8 GHz, in Joule annealed Co-based amorphous microwires. It is shown that the crystallization process can be followed by the evaluation of the extrinsic magnetization damping terms, specifically analyzing contributions from inhomogeneities to the FMR linewidth. From the fitting of models which consider LL damping term, anisotropy dispersion and magnon scattering to the experimental data, three ranges of annealing temperatures can be distinguished in terms of spin dynamics on the studied samples: annealing temperatures lower than the Curie temperature, a temperature range between the Curie and the crystallization temperature and another temperature range above the crystallization temperature.

© 2013 Elsevier B.V. All rights reserved.

## 1. Introduction

Magnetoimpedance has been proved to be an excellent tool to study the magnetization dynamics while the ferromagnetic resonance (FMR) linewidth provides a convenient way for measuring damping parameters associated to the magnetization precession in magnetic materials [1–5]. The ferromagnetic resonance linewidth depends on the intrinsic magnetic damping and additional magnetic inhomogeneities, but the complete understanding of the origin of these damping parameters is still unaccomplished. Besides the fundamental physics interest, the study of the damping term and the magnetization dynamics are very important to the development of any device which has its physical effect associated to the reversal of the magnetization [6,7]. In addition, the FMR linewidth ( $\Delta f_R$ ) is a very sensitive way to study the structural quality of magnetic samples, in both bulk [2] and thin films [1] geometries.

The magnetic properties of the amorphous materials are correlated with their microstructure, composition and internal stresses originated from the fabrication processes. By annealing the microwires all of the above aspects can be modified, being

this the main advantage of this kind of materials, meaning that the magnetic properties can be tailored to a particular application by a proper annealing [8,9].

This work shows measurements of magnetoimpedance based FMR linewidth in CoFeSiB glass-covered microwires, under different annealing temperatures in order to investigate the influence coming from different sources of inhomogeneities, namely: anisotropy dispersion and magnon scattering. In addition to the previous work [3], it is possible to observe the crystallization processes by means of the FMR linewidth.

## 2. Experimental

The as-cast microwires were produced by the Taylor–Ulitovski technique with nominal composition  $\text{Co}_{68.15}\text{Fe}_{4.35}\text{Si}_{12.5}\text{B}_{15}$ , having diameters of  $\phi_m \sim 25 \mu\text{m}$  (amorphous metallic nucleus) and  $\phi_t \sim 44 \mu\text{m}$  (total). These samples present a low and negative magnetostriction and the magnetic characterization have already been described, for example, in [10,11]. The studied microwires were Joule-annealed at different DC currents from 16.5 mA to 72 mA during 60 min, corresponding to the estimated temperatures from 150 °C to 750 °C [12], respectively. The samples were all cut in pieces of 16 mm in length.

\* Corresponding author. Tel.: +55 55 3220 8888; fax: +55 55 3220 8032.

E-mail addresses: [marcos.carara@gmail.com](mailto:marcos.carara@gmail.com), [carara@mail.ufsm.br](mailto:carara@mail.ufsm.br) (M. Carara).

The room temperature impedance measurements were performed as function of frequency ( $100 \text{ kHz} \leq f \leq 1.8 \text{ GHz}$ ) and magnetic field ( $-300 \leq H \leq 300 \text{ Oe}$ ) parallel to the wire's axis, using an HP4396B impedance analyzer with a HP4396A1 impedance test kit and a proper calibration of the system, with the open, short and load standards. For all the measurements, a 0 dBm (1 mW) constant power was applied to the sample. At each set field value, a frequency sweep was performed and the real ( $R$ ) and imaginary ( $X$ ) part of the impedance were simultaneously acquired. From this impedance spectrum, the circumferential permeability curves were extracted according to the procedure described in Ref. [13]. Finally, from the permeability curves, the ferromagnetic resonance frequency ( $f_R$ ), the resonance linewidth ( $\Delta f_R$ ) and the amplitude of the rotational contribution to the circumferential permeability ( $\mu_{\text{rot}}$ ) were obtained.

Magnetization curves of the studied samples were performed at room temperature in a vibrating sample magnetometer with the applied field along the samples' axis and ranging from  $-20 \text{ Oe}$  to  $20 \text{ Oe}$ . It is worth to note that in the VSM and impedance analyzer measurements the very same samples were used.

### 3. Results and discussion

In a previous work [3] the different contributions to  $\Delta f_R$  were described, being briefly discussed here.

The inhomogeneities coming from the exciting  $rf$  field [1] can be neglected here as the  $rf$  field is that related to the impedance measurement current. Associated to the cylindrical shape of the samples this field is circumferential and homogeneous over the whole surface of the sample. Another disregarded damping term is that associated to the eddy currents [5]. The procedure to obtain the permeability from the impedance data consider that the skin effect is the linking phenomena, so the eddy current term is already accounted in the permeability data. The simplicity which arises from the absence of these two effects can be considered as an advantage to study the magnetization dynamics via impedance measurements in wires.

Finally, the damping terms considered in this work are the Gilbert like damping term, the local resonance contributions coming from the anisotropy dispersion and the magnon scattering.

The Gilbert term is due to the exchange interaction and the spin–orbit coupling [2]. In the work of Suhl [15] on FMR, a relation for the field linewidth has been described and, in terms of frequency ( $\Delta f_R^G$ ), it can be expressed as

$$\Delta f_R^G = \frac{\gamma\alpha}{2\pi} [2H + 4\pi M_S - H_K], \quad (1)$$

where  $M_S$  is the saturation magnetization and  $H_K$  the circumferential anisotropy field which, in the studied samples, is orthogonal to the applied one. From (1) it can be seen that the resonance linewidth increases linearly with the applied field. Fig. 1 shows a typical example of the experimental data and the dashed line in the figure represents the Gilbert contribution to the total damping.

Any dispersion in the sample's anisotropy would give rise to local resonances resulting in an additional broadness to the FMR linewidth. As different portions of the sample resonate in slightly different frequencies, these will result in a larger FMR line [16]. Assuming that the FMR dispersion relation of a material with an uniaxial anisotropy orthogonally aligned to the applied field can be described by the Kittel's relation [17], the enlargement in the resonance line associated to dispersion in the anisotropy amplitude ( $\Delta f_R^K$ ) can be described as

$$\Delta f_R^K = \frac{\Delta H_K}{f_R} \left( \frac{\gamma}{2\pi} \right)^2 (H - H_K + 2\pi M_S), \quad \text{for } H > H_K. \quad (2)$$

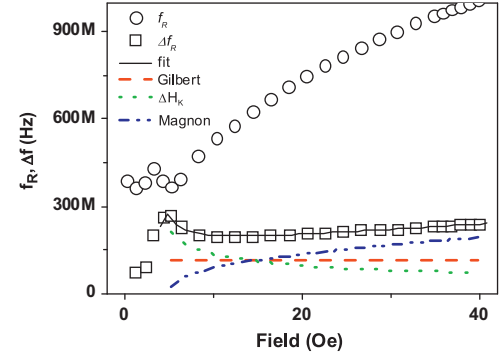


Fig. 1. Field evolution of the resonance frequency ( $\square$ ) and frequency linewidth ( $\circ$ ) of the as cast sample. Field dependency of each contribution to the FMR frequency linewidth: dashed line—Gilbert damping; dotted line—anisotropy dispersion; dash-dotted line—magnon scattering; solid line—geometrical sum of the three damping components.

From the expression (2) it can be seen that the main feature of the anisotropy dispersion to the FMR linewidth is a maximum at  $H = H_K$ , field in which  $f_R$  is minimum for the studied system with circumferential anisotropy (represented by the dotted line in Fig. 1). The  $\Delta H_K$  value quantifies the anisotropy dispersion.

In a FMR experience, at the resonance frequency it is assumed that all samples' spins precesses in an uniform mode (wave vector  $\mathbf{k} = 0$ ). However, the inhomogeneities in the sample can scatter a magnon of frequency  $f$  and  $\mathbf{k} = 0$  in another one with the same  $f$  but with  $\mathbf{k} \neq 0$ . This will result in an additional contribution to the FMR linewidth [1]. The inhomogeneities can be, for example, small variations on the local effective field, additional phases, pores, surface pits and so on [18]. In order to formulate a complete analysis of magnon scattering on the FMR linewidth it would be required to describe the magnon dispersion relation and to know how each inhomogeneity contribute to the scattering. A detailed study on the subject, applied to thin films, can be found in [19], where the authors have considered dipolar interaction, Zeemann, exchange and surface anisotropy energies. As scattering elements, rectangular islands and pits were considered. Although the magnon scattering contribution to the FMR linewidth can be calculated for this particular thin film case, Arias and Mills [19] state that the signature of the magnon scattering is a term proportional to  $\sin^{-1}[\sqrt{H/(B+H_K)}]$ , which has its origin on the nature of the spin-wave dispersion and it is not influenced by the details of the scattering matrix. The following expression is suggested to fit the data:

$$\Delta f_R^{MS} = \gamma P_A(f) \Gamma_S(H) \sin^{-1} \sqrt{\frac{H - H_K}{H + 4\pi M_S - 2H_K}}, \quad (3)$$

where the term  $P_A(f) = \sqrt{1 + (|\gamma| \mu_0 M_S / 4\pi f)^2}$  is a conversion factor used to switch from field linewidth to frequency linewidth [20], for a film with an in plane easy axis.  $\Gamma_S$  is a parameter who quantifies the intensity of the magnon scattering. Dash-dotted line in Fig. 1 accounts for the magnon contribution to the total damping.

As each of the described damping terms presents a different behavior with the applied magnetic field, the analysis of the field dependency of the  $\Delta f_R$  allow to separate the contributions from the above discussed sources of enlargement to the  $\Delta f_R$  and to evaluate their evolution with the annealing temperature [21].

The fitting procedure is made in steps; first  $M_S$  and  $H_K$  are obtained from the  $f_R$  vs.  $H$  data, as already described in Ref. [22] and, with these parameters held constant, the  $\Delta f_R$  data are fitted to the above discussed theory. The fittings were made for  $H > H_K$

as shown in Fig. 1 for the as cast sample. It can be verified that the above discussed model fits very well the experimental data.

Fig. 2 shows the magnetization curves of some of the studied samples. All of them have the same length, 16 mm, but the samples with  $I_{ann} < 35$  mA present a strong effect of the demagnetizing field. The magnetic structure of these samples is that called core-shell, meaning an axial magnetized core, surrounded by a circumferential shell. Usually such materials present a bistable behavior, but for these samples with reduced length the demagnetizing field influences both nucleation and propagation of the magnetization reversal, resulting in a change of hysteresis loop shape [23]. In the samples annealed at the higher currents ( $I_{ann} \geq 35$  mA) the magnetization curves present an increase in both, coercive field and saturation fields which is a manifestation of a hardening of the magnetic properties, probably coming from the crystallization of the samples.

Fig. 3(a) shows the evolution with the current annealing of the magnetoimpedance  $[\Delta Z(H)/Z(H_{max}) \times 100\%]$  measured at 8 MHz. This frequency is high enough to prevent a major contribution of the circumferential domain wall to the permeability and low enough to the measuring current probe the entire cross section of the samples. In this way the only contribution to the permeability present in the MI measurement comes from the rotation of the magnetization.

By analyzing the MI curves, it can be seen that a double-peak structure is present just in the as cast sample. This behavior is typical for a permeability of a magnetic system measured in the presence of a dc bias field along the hard axis, meaning that the contribution of the circumferential shell is present in the MI curve for this sample. For the annealed samples a single peak character dominates the MI spectrum. For these samples the relaxation in the frozen stress was high enough to reduce the thickness of the circumferential shell and its contribution to the shape of the MI curves. On the other hand, as can be seen in Fig. 3(b) the transverse permeability increases with the annealing current until  $I_{ann} < 45$  mA, showing that the anisotropy is reduced in this range of annealing. The further increase in  $I_{ann}$  promotes the

growing of crystallites in the samples which, by its time, increase the anisotropy and as a consequence reduces the MI ratio.

The resonance linewidth of some of the samples is presented in Fig. 4 superposed to the fitting obtained with the model above described. The trending of  $\Delta f_{res}$  to increase with the applied field

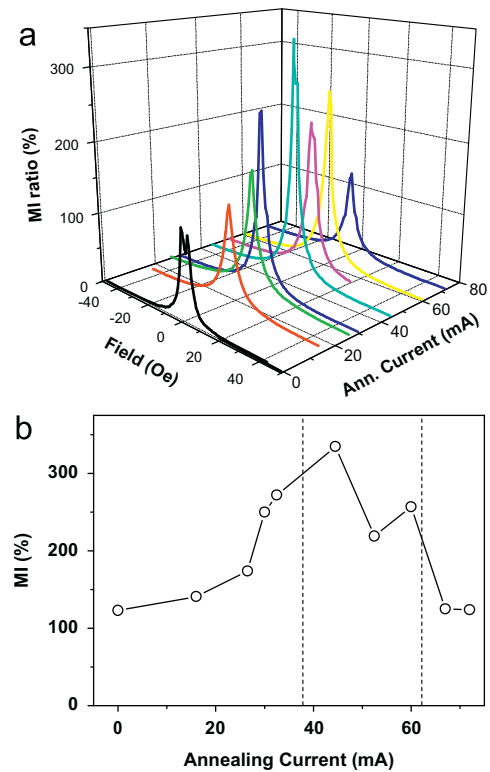


Fig. 3. (a) MI ratio as function of the applied field measured at 8 MHz for the different annealing currents. (b) Annealing current evolution of the maximum of the MI ratio.

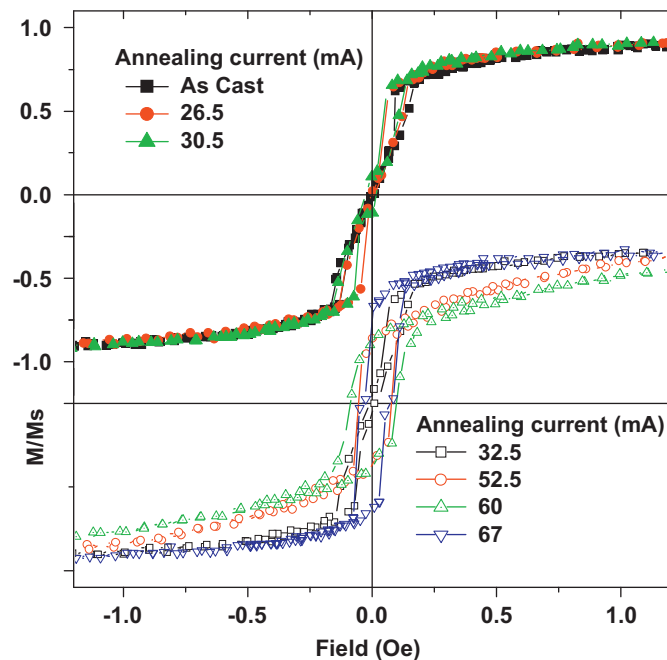


Fig. 2. Magnetization curves obtained from the studied samples. (a) As cast sample, annealed at 32.5 mA (b), 52 mA (c) and (d) 60 mA. The equivalent temperatures of these currents are, respectively, 300 °C, 450 °C and 500 °C. The samples are the same used in the impedance measurements.

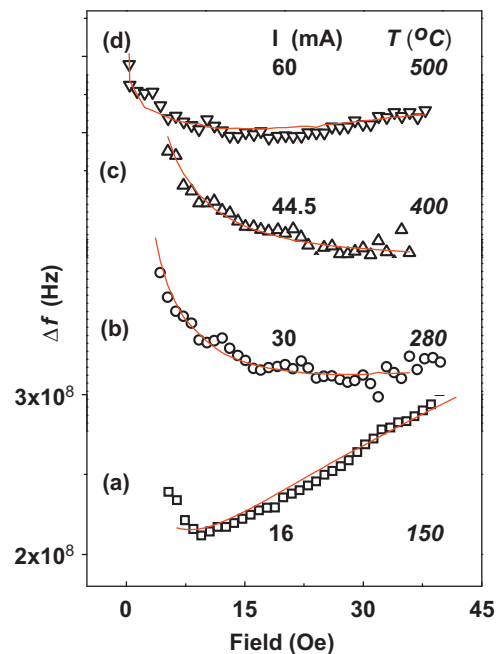


Fig. 4. Resonance frequency linewidth vs. applied field, measured from the Joule annealed microwire at the currents (equivalent temperatures) indicated in the figure. Symbols represent the experimental data and solid line is the fitting as described in the text.

is typical of the Gilbert damping and the magnon scattering contribution to the total relaxation. It can be clearly seen that these contributions are less representative in the samples annealed at 30 and 44 mA. From the data presented in Fig. 4, without the fitting, it is hard to infer how great the anisotropy dispersion is. The scenario becomes clearer when the fitting parameters are plotted vs. the annealing current, as can be seen in Figs. 5 and 6.

The saturation magnetization and the Gilbert contribution to the spin relaxation present almost no changes with the annealing current and the values obtained from the fitting were  $M_S \sim 9.000$  G and  $\alpha \sim 0.014$ . Fig. 5 shows the evolution of the anisotropy field and the anisotropy dispersion with the annealing current. It is worth to note that the resonance frequency dispersion was fitted to a core-shell magnetic structure, with a negative anisotropy field in the shell and a positive one in the core. The fitting procedure of this kind of structure can be found better discussed in Ref. [22]. The opposite sign of anisotropy field of both wire's region explain the higher value of the anisotropy dispersion when compared to the anisotropy field values. The anisotropy field values of both, inner core ( $H_{KI}$ ) and outer shell ( $H_{KO}$ ), present a small reduction in its values until 26 mA. This reduction in the anisotropy fields are higher in the range between 26 and 32 mA, from where they start to increase. The anisotropy

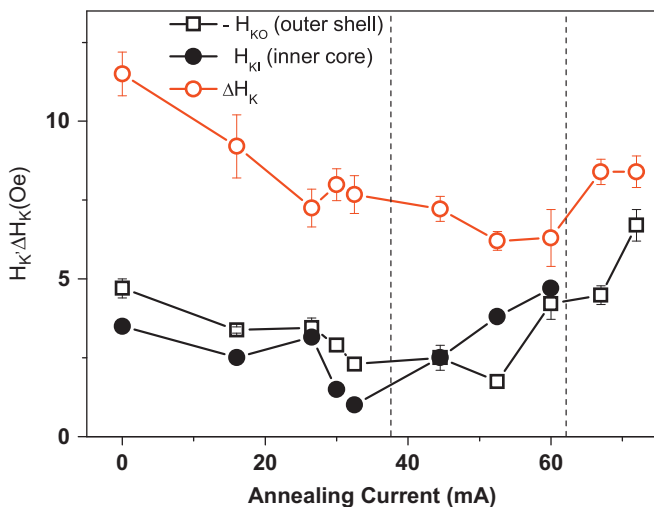


Fig. 5. Anisotropy Fields of the inner core ( $H_{KI}$ ) and outer shell ( $H_{KO}$ ) portions of the samples as function of the annealing current. Open circles represent the anisotropy dispersion contribution to the FMR linewidth for the studied samples.

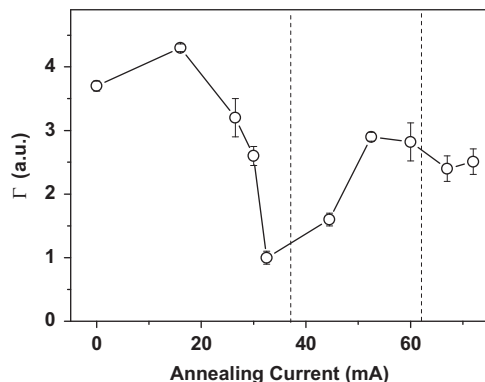


Fig. 6. Two-magnon scattering contribution to the FMR linewidth, as a function of the applied stress for all studied samples.

dispersion also presents a trend of reduction in its values until  $\sim 50$  mA, from where it starts to increase.

The most significant evolution with the annealing current, together with the MI ratio, is that one presented by the magnon scattering contribution to the FMR linewidth ( $\Gamma_S$ ) shown in Fig. 6. The  $\Gamma_S$  value is strongly reduced between 26 and 32 mA, then it increases until 52 mA, followed by a range of annealing currents (between 52 and 72 mA) with almost no  $\Gamma_S$  variation.

As also discussed by other authors [8,9], the annealing of this kind of amorphous samples is frequently used to tailor its magnetic properties. As reported in [24] the Curie and crystallization temperature of samples with the same composition of the samples studied in this work are, respectively, 343 °C and 510 °C, or in equivalent current 38 and 62 mA. Such annealing currents are signed as vertical dashed lines in Figs. 3(b), 5 and 6. In addition, it must be remembered that the Joule heating is an annealing process with magnetic applied field, the Oersted one. At the metallic surface of the samples, with an annealing current of 30 mA, the Oersted field is around 5 Oe, comparable to the anisotropy ones.

The magnon scattering reveals that the annealing with currents between 16 and 30 mA reduces the inhomogeneities, coming from the anisotropy dispersion (due to the Oersted field annealing) and reduction of the internal frozen stress. The fluctuations of the local fields coming from different regions of the sample lead to a coupling between the driven mode and the available spin-wave modes at the same frequency.

The further increase in the annealing current promotes the crystallization of small grains in the sample embedded in the amorphous ferromagnetic matrix [25,26]. The formation of these crystallites acts as scattering centers for the magnons and, as the annealing current increases, such crystallites increase the number and average size. In Ref [27] the authors present theoretical results on magnon scattering contribution to the FMR linewidth, showing that magnon scattering is strongly influenced by the size of the grain.

#### 4. Conclusions

We have investigated the magnetization dynamics during the devitrification process of CoFeSiB glass-covered microwire. The study was made by the analysis of the FMR linewidth measurements assuming that the main mechanisms responsible for the magnetic relaxation are the Gilbert like damping term, local resonance contributions coming from the anisotropy dispersion and two-magnon scattering. The fitting of the theory associated to the magnetization dynamics to the experimental data has shown that the Gilbert damping term was almost constant and not influenced by the annealing. The anisotropy dispersion evolution with the annealing current, initially ( $I_{ann} < 26$  mA) reduces its value being accompanied by the reduction of the magnon scattering contribution to the total damping. This fact is a reflex of an increase in the homogeneity of the stress distribution. By annealing at higher currents ( $I_{ann} > 32$  mA) the crystallization process takes place. Initially with small grains which grows in size and number as the annealing current is increased. The grain boundaries act as scattering centers to the magnons promoting an additional increase in the FMR linewidth and quantified by the increase in the  $\Gamma_S$  parameter.

#### Acknowledgments

This work was partially supported by the Brazilian agencies, CNPq (Conselho Nacional de Desenvolvimento Científico e

Tecnológico), CAPES (Coordenação de Aperfeiçoamento de Pessoal de Nível Superior) and FAPERGS (Fundação de Amparo à Pesquisa do Rio Grande do Sul). The authors thank Prof. H. Chiriac, from National Institute and Development for Technical Physics, Iasi, Romania, for supplying the studied samples.

## References

- [1] M.J. Hurben, C.E. Patton, *Journal of Applied Physics* 83 (1998) 4344.
- [2] L. Kraus, Z. Frait, *Czechoslovak Journal of Physics* 21 (1971) 979.
- [3] K.D. Sossmeier, F. Beck, R.C. Gomes, L.F. Schelp, M. Carara, *Journal of Physics D: Applied Physics* 43 (2010) 055003.
- [4] L. Kraus, M. Vázquez, G. Infante, G.B. Confalonieri, J. Torrejon, *Applied Physics Letters* 94 (2009) 62505.
- [5] W.S. Ament, G.T. Rado, *Physical Review* 97 (1955) 1558.
- [6] D.A. Alwood, G. Xiong, C.C. Faulkner, D. Atkinson, D. Petit, R.P. Cowburn, *Science* 309 (2005) 1688.
- [7] S.S.P. Parkin, H. Masamitsu, L. Thomas, *Science* 320 (2008) 209.
- [8] V.S. Larin, V. Zhukova, A. Zhukov, A.V. Torcunov, M. Vázquez, *Sensors and Actuators A* 106 (2003) 96.
- [9] J. Arcas, C.G. Polo, A. Zhukov, M. Vázquez, V. Larin, A. Hernando, *Nanostructured Materials* 7 (1996) 823.
- [10] H. Chiriac, M. Neagu, M. Vázquez, T.A. Óvári, E. Hristoforou, *Journal of Magnetism and Magnetic Materials* 249 (2002) 122.
- [11] K.R. Pirota, R. Kaus, H. Chiriac, M. Knobel, *Journal of Magnetism and Magnetic Materials* 221 (2000) 243.
- [12] H. Chiriac, M. Knobel, T.A. Óvári, *Materials Science Forum* 302 (1999) 239.
- [13] K.D. Sossmeier, G.L. Callegari, L.S. Dorneles, M. Carara, *Journal of Magnetism and Magnetic Materials* 320 (2008) e1.
- [15] H. Suhl, *Physical Review* 97 (1955) 555.
- [16] D.-de Cos, A.-A. García, J.M. Barandiaran, *Journal of Magnetism and Magnetic Materials* 320 (2008) 2513.
- [17] C. Kittel, *Quantum Theory of Solids*, John Wiley and Sons, New York, 1963.
- [18] S.S. Kalarickal, N. Mo, P. Krivosik, C.E. Patton, *Physical Review B* 79 (2009) 94427.
- [19] R. Arias, D.L. Mills, *Physical Review B* 60 (1999) 7395.
- [20] S.S. Kalarickal, P. Krivosik, M. Wu, C.E. Patton, M.L. Schneider, P. Kabos, T. Silva, J.P. Nibarger, *Journal of Applied Physics* 99 (2006) 093909.
- [21] H. Lee, Y.H.A. Wang, C.K.A. Mewes, W.H. Butler, T. Mewes, S. Maat, B. York, M.J. Carey, J.R. Childress, *Applied Physics Letters* 95 (2009) 082502.
- [22] M. Carara, K.D. Sossmeier, A.D.C. Viegas, J. Geshev, H. Chiriac, R.L. Sommer, *Journal of Applied Physics* 98 (2005) 033902.
- [23] M. Vazquez, C.-P. Gomez, D.-X. Chen, A. Hernando, *IEEE Transactions on Magnetics* 30 (1994) 907.
- [24] S.M. Hoque, A.K.M. Haque, M.O. Rahman, N.H. Nghi, M.A. Hakim, S. Akhter, *Journal of Non-Crystalline Solids* 357 (2011) 2109.
- [25] C.-P. Gómez, M. Vázquez, *Journal of Magnetism and Magnetic Materials* 118 (1993) 86.
- [26] G. Buttino, A. Cecchetti, M. Poppi, *Journal of Magnetism and Magnetic Materials* 172 (1997) 147.
- [27] R.D. McMichael, D.J. Twisselmann, A. Kunz, *Physical Review Letters* 90 (2003) 227601.